



NRL/MR/6703--15-9643

Optical Magnetometry for Detecting Underwater Objects

ZACHARY EPSTEIN

*University of Maryland
College Park, Maryland*

PHILLIP SPRANGLE

*Directed Energy Physics
Plasma Physics Division*

September 21, 2015

Optical Magnetometry for Detecting Underwater Objects

Zachary Epstein¹ and Phillip Sprangle

Plasma Physics Division
Naval Research Laboratory
Washington DC 20375

¹University of Maryland
College Park, MD 20742-4111

Abstract

A method for remote optical measurements of magnetic field variations above the surface of seawater is analyzed. This magnetometry mechanism is based on the fact that polarized laser light, in the presence of the Earth's magnetic field, will exhibit a polarization rotation when reflected off the surface of the water and off an underwater object. The two mechanisms responsible for the polarization rotation are the Surface Magneto-Optical Kerr Effect (SMOKE) and the Faraday effect. In both mechanisms, the degree of polarization rotation is proportional to Earth's local magnetic field. Variations in the Earth's magnetic field due to an underwater object will result in variations in the polarization rotation of the laser light reflected off the water's surface (SMOKE) and off the underwater object itself (Faraday effect). An analytical expression is obtained for the polarization-rotated field when the incident plane wave is at arbitrary angle and polarization with respect to the water's surface.

I. Introduction

Optical magnetometry can be a highly sensitive method for measuring small variations in magnetic fields [1-3]. The development of a remote optical magnetometry system would have important applications for the detection of underwater and underground objects that perturb the local ambient magnetic field. For a number of magnetic anomaly detection (MAD) applications, μG magnetic field variations must be detected at standoff distances greater than 10^2 m from the sensor [4-5]. The remote atmospheric optical magnetometry mechanism considered here is based on polarization changes in reflected laser light from the surface of sea water.

The dielectric properties of water in the presence of a magnetic field will rotate the polarization of an optical field. The polarization rotation occurs via two distinct mechanisms: the Surface Magneto-Optical Kerr Effect (SMOKE) and the Faraday rotation effect. SMOKE is purely a surface phenomenon in which the degree of polarization rotation of the reflected light is proportional to the magnetic field but not to the propagation distance in the water [6]. The SMOKE mechanism is used in material science research in such devices as the Kerr microscope. The Faraday effect is due to the difference in propagation speed of right-hand and left-hand polarized light, and the resulting degree of polarization rotation is proportional to both, the magnetic field and the propagation distance.

In this paper, we consider whether these effects can be used for the remote detection of underwater objects. An underwater object can produce appreciable magnetic field perturbations above the water's surface. The proposed magnetometry mechanism is shown schematically in Fig. 1. Here, a linearly-polarized laser beam is propagated to and reflects off the water's surface near the detection site. The degree of polarization rotation in the reflected field is proportional to the local magnetic field. The magnitude of the polarization-rotated component of the reflected field is measured at various locations near the inspection site. An irregularity in the measurement at one location would correspond to a deviation in the local magnetic field. The local field deviation could indicate the presence of an underwater object.

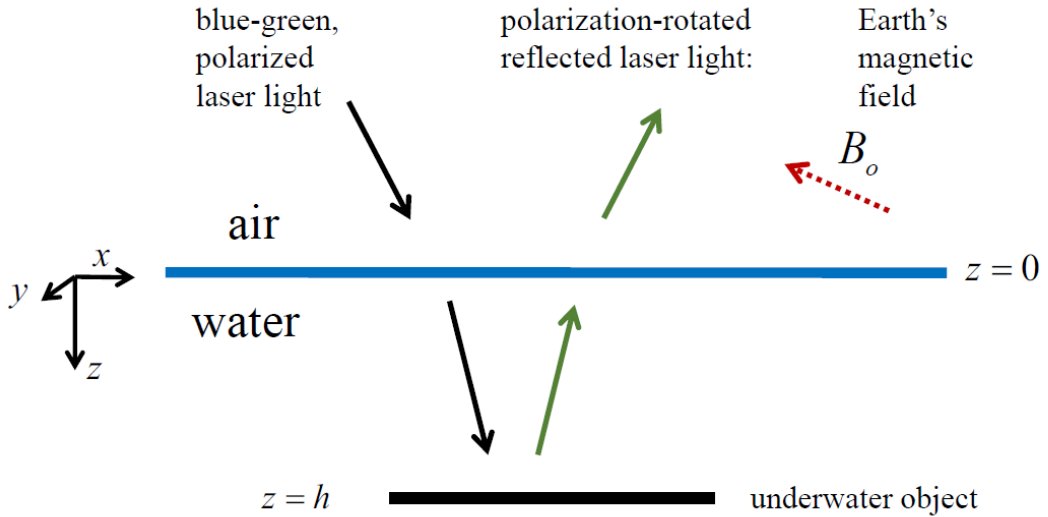


Figure 1: Polarized laser light is propagated to the surface of the water and exhibits polarization rotation upon reflection due to Faraday rotation and SMOKE. The purpose of this paper is to estimate the polarization rotation angle $\Delta\theta \propto B_0$. If $\Delta\theta$ is large enough to be precisely measured, the mechanism shown in this figure enables the measurement of fluctuations in the Earth's magnetic field B_0 , which in turn may indicate the presence of an underwater object. The solid arrows in the figure denote wave vectors.

II. Model

To analyze the Surface Magneto-Optical Kerr and the Faraday rotation effects, we first obtain the dielectric properties of magnetized, pure water. The polarization field associated with magnetized water at the laser frequency is obtained using an extended form of the Lorentz model [7]. The polarization field is used to derive a wave equation for the reflected laser field. By appropriately matching boundary conditions at the various interfaces, we obtain the reflected field which has its polarization modified by both, the SMOKE and Faraday effect. The polarization-rotated component of the field is proportional to the local magnetic field. In applying the boundary conditions, the laser propagation direction and polarization as well as the Earth's magnetic field are taken to be in an arbitrary direction.

i) **Polarization Field of Magnetized Water**

In the Lorentz model, the dielectric properties of the molecule are represented by the motion of the forced displacement of the electron distribution from its equilibrium position. The

displacement of the electron distribution $\delta r(\mathbf{r}, t)$ is modeled by the following driven harmonic oscillator equation,

$$\left(\frac{\partial^2}{\partial t^2} + \Omega_B^2 + \gamma \frac{\partial}{\partial t} \right) \delta \mathbf{r} = \frac{q}{m} \left(\mathbf{E} + \frac{\partial \delta \mathbf{r}}{\partial t} \times \mathbf{B}_o / c \right), \quad (1)$$

where Ω_B is the electron binding frequency, γ is the damping coefficient, q is the electronic charge, m is the electronic mass, and \mathbf{B}_o is the local magnetic field, i.e., Earth's magnetic field ~ 0.5 G. The laser electric field is $\mathbf{E}(\mathbf{r}, t) = \text{Re}(\hat{\mathbf{E}}(\mathbf{r}) \exp(-i \omega t))$ where ω is the frequency.

The magnetic field associated with the laser is neglected on the right hand side of Eq. (1) since it produces forces at frequencies of 2ω and 0.

The polarization field associated with the magnetized water molecules is given by $\hat{\mathbf{P}}(\mathbf{r}) = qN\delta\hat{\mathbf{r}}$, where $\delta\hat{\mathbf{r}}(\mathbf{r})$ represents the electronic displacement from equilibrium of the water molecule, N is the effective bound electron density of the water molecules, and phasor notation is used throughout to represent the various field quantities, i.e., $\mathbf{Q}(\mathbf{r}, t) = \text{Re}(\hat{\mathbf{Q}}(\mathbf{r}) \exp(-i \omega t))$. The displacement $\delta\hat{\mathbf{r}}(\mathbf{r})$ is given by

$$(-\omega^2 + \Omega_B^2 - i\gamma\omega)\delta\hat{\mathbf{r}}(\mathbf{r}) = q(\hat{\mathbf{E}}(\mathbf{r}) - i\omega\delta\hat{\mathbf{r}}(\mathbf{r}) \times \mathbf{B}_o / c) / m. \quad (2)$$

The polarization field, correct to first order in the magnetic field, is

$$\hat{\mathbf{P}}(\mathbf{r}) = qN\delta\hat{\mathbf{r}} \approx \frac{\omega_{pN}^2}{4\pi D(\omega)} (\hat{\mathbf{E}}(\mathbf{r}) + i\omega\Omega_o \times \hat{\mathbf{E}}(\mathbf{r}) / D(\omega)), \quad (3)$$

where $D(\omega) = \Omega_B^2 - \omega^2 - i\gamma\omega$, $\omega_{pN} = (4\pi q^2 N / m)^{1/2}$, and $\Omega_0 = qB_0 / mc \sim 10^7 s^{-1}$.

The laser frequency is chosen to be in the blue-green range where the penetration depth is maximum. In the following examples, the laser frequency is taken to be $\omega = 3.8 \times 10^{15}$ rad/s ($\omega = 2.48 \text{ eV}/\hbar$) where pure water's absorption coefficient is minimum, i.e., $\alpha = 5 \times 10^{-4} \text{ cm}^{-1}$; the corresponding penetration depth (e-folding length) is $h_e \approx 20 \text{ m}$. In the blue-green regime, the real part of the refractive index is $\text{Re}[n_0] \approx 1.34$. The lowest energy electron-binding frequency in water is $\Omega_B \approx 23.5 \text{ eV}/\hbar$, $\omega_{pN} \approx 21 \text{ eV}/\hbar$, and the damping coefficient is $\gamma \approx 3 \times 10^9 \text{ s}^{-1}$.

In general, there are many resonances above Ω_b which contribute to the refractive index of water. We neglect these binding frequencies since they are at higher energies. In addition, the oscillator strength parameter associated with the Ω_b resonance is taken to be unity [8]. Nonlinear effects in water can be neglected since the laser intensity is well below the level where these become important.

ii) Wave Equation

In the absence of free charges and currents, Maxwell's equations for the fields in phasor notation are given by $\nabla \times \hat{\mathbf{H}} = -i(\omega/c)\hat{\mathbf{D}}$, $\nabla \cdot \hat{\mathbf{D}} = 0$, $\nabla \times \hat{\mathbf{E}} = i(\omega/c)\hat{\mathbf{B}}$ and $\nabla \cdot \hat{\mathbf{B}} = 0$. These equations can be combined to give

$$\nabla^2 \hat{\mathbf{E}} + (\omega^2/c^2)\hat{\mathbf{D}} = \nabla(\nabla \cdot \hat{\mathbf{E}}). \quad (4)$$

To obtain a wave equation for $\hat{\mathbf{E}}$, we note that the electric flux density $\hat{\mathbf{D}} = (\hat{\mathbf{E}} + 4\pi\hat{\mathbf{P}})$ is given by $\hat{\mathbf{D}} = (\epsilon_o + i(\epsilon_o - 1)(\omega/D(\omega))\boldsymbol{\Omega}_o \times) \hat{\mathbf{E}}$, where the electric polarization field is given in Eq. (3) and where the dielectric constant of water, in the absence of the Earth's magnetic field, is $\epsilon_o(\omega) = 1 + \omega_{PN}^2/D(\omega)$. Since $\nabla \cdot \hat{\mathbf{D}} = 0$, we find that

$$\nabla \cdot \hat{\mathbf{E}} = -i \frac{(\epsilon_o - 1)}{\epsilon_o} \frac{\omega}{D(\omega)} \nabla \cdot (\boldsymbol{\Omega}_o \times \hat{\mathbf{E}}) = i \frac{(\epsilon_o - 1)}{\epsilon_o} \frac{\omega}{D(\omega)} (\boldsymbol{\Omega}_o \cdot (\nabla \times \hat{\mathbf{E}})), \quad (5)$$

where the final form for $\nabla \cdot \hat{\mathbf{E}}$ is valid since $\boldsymbol{\Omega}_o$ is spatially uniform. Using Eqs. (4) and (5), the wave equation takes the form

$$\nabla^2 \hat{\mathbf{E}} + \epsilon_o \frac{\omega^2}{c^2} \hat{\mathbf{E}} = -i \frac{\omega^2}{c^2} (\epsilon_o - 1) \frac{\omega}{D(\omega)} (\boldsymbol{\Omega}_o \times \hat{\mathbf{E}}) + i \frac{(\epsilon_o - 1)}{\epsilon_o} \frac{\omega}{D(\omega)} \nabla(\boldsymbol{\Omega}_o \cdot (\nabla \times \hat{\mathbf{E}})), \quad (6)$$

The right-hand side of Eq. (6) can be simplified by noting that

$$\nabla(\boldsymbol{\Omega}_o \cdot (\nabla \times \hat{\mathbf{E}})) = \boldsymbol{\Omega}_o \times (\nabla \times \nabla \times \hat{\mathbf{E}}) + (\boldsymbol{\Omega}_o \cdot \nabla)(\nabla \times \hat{\mathbf{E}}) \text{ and, to lowest order in } \boldsymbol{\Omega}_o,$$

$\nabla \times \nabla \times \hat{\mathbf{E}} = (\omega^2/c^2)\epsilon_o \hat{\mathbf{E}}$. The final form for the wave equation, correct to first order in $\boldsymbol{\Omega}_o$, is

$$\left(\nabla^2 + \epsilon_o \frac{\omega^2}{c^2} \right) \hat{\mathbf{E}} = i \frac{(\epsilon_o - 1)}{\epsilon_o} \frac{\omega}{D(\omega)} (\boldsymbol{\Omega}_o \cdot \nabla)(\nabla \times \hat{\mathbf{E}}). \quad (7)$$

Since the right-hand side of Eq. (7) is small, we can write the total field as $\hat{\mathbf{E}}(\mathbf{r}) = \hat{\mathbf{E}}_o + \delta\hat{\mathbf{E}}$, where $\hat{\mathbf{E}}_o$ here denotes the laser field in the absence of the perturbation (i.e. the Earth's magnetic

field) and $\delta\hat{\mathbf{E}}$ is the small polarization-modified component of the laser field due to the Earth's magnetic field and driven by the laser field $\hat{\mathbf{E}}_o$. Separate wave equations can be written for these fields:

$$\left(\nabla^2 + \varepsilon_o \frac{\omega^2}{c^2}\right)\hat{\mathbf{E}}_o = 0, \quad (8a)$$

$$\left(\nabla^2 + \varepsilon_o \frac{\omega^2}{c^2}\right)\delta\hat{\mathbf{E}} = i \frac{(\varepsilon_o - 1)}{\varepsilon_o} \frac{\omega}{D(\omega)} (\mathbf{\Omega}_o \cdot \nabla)(\nabla \times \hat{\mathbf{E}}_o). \quad (8b)$$

In the special case where the laser field \mathbf{E}_o is transverse to the magnetic field \mathbf{B}_o , one can recover from Eq. (8b) the usual Faraday rotation angle, i.e.

$$\Delta\theta_F \approx \omega_{pN}^2 \omega^2 \Omega_0 L / (2c \Omega_B^4) \square (10^{-4} \text{G}^{-1} \text{m}^{-1} \text{rad}) L B_o, \text{ where } L \text{ is the propagation distance [9].}$$

These wave equations are numerically solved for arbitrary laser field propagation direction, polarization and magnetic field direction.

III. Analysis of Polarization Rotation

The proposed magnetometry method is feasible only if the laser beam's polarization rotates a substantial amount upon reflection off the water's surface. The purpose of the analysis is thus to calculate the amount of polarization rotation $\Delta\theta = |\delta E|/|E_{r1}|$, where δE is the polarization-rotated component of the reflected laser field and E_{r1} is the un-rotated component. Alternatively, this is written as $\Delta\theta = (1/R)|\delta E|/|E_0|$, where E_0 is the incident laser field and the reflection coefficient is $R = (n-1)/(n+1) \approx 0.15$.

We first consider a simplified configuration as shown in Fig. 2 to obtain estimates for the amount of polarization rotation $\Delta\theta$. Here a linearly-polarized, monochromatic laser beam is propagated parallel to Earth's magnetic field which is taken to be perpendicular to the surface of the water. An optically reflective underwater object at depth h below the water's surface is represented by a perfectly conducting plate parallel to the surface.

From this simplified configuration will emerge two distinct contributions to the polarization rotation: the Faraday effect and SMOKE. The Faraday effect yields the ratio $|\delta E/E_0| \sim 12\pi n_0 h \xi/\lambda$, whereas SMOKE yields $|\delta E/E_0| \approx \xi \square 3 \times 10^{-12}$. The Faraday effect is larger by the ratio $h/\lambda \square 1$.

The SMOKE contribution to the polarization rotation is obtained for an arbitrary configuration.

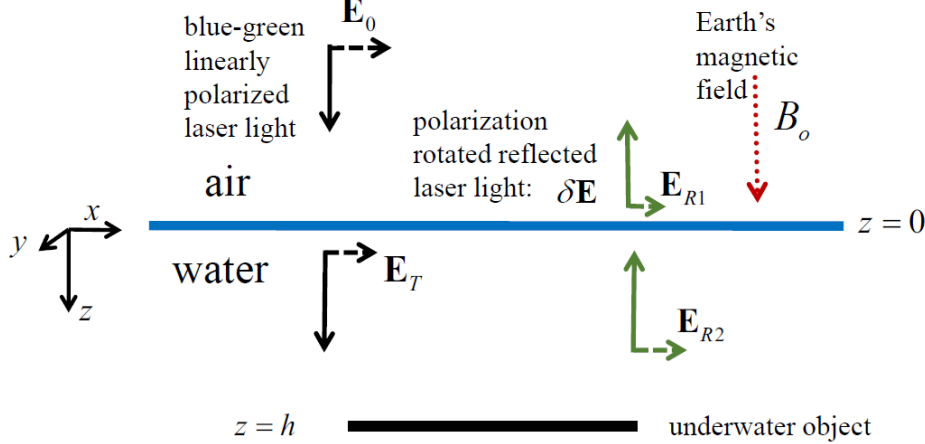


Figure 2: A simple, geometrical configuration of reflected laser light undergoing polarization rotation due to Faraday rotation and SMOKE. The purpose of this configuration is to obtain estimates for the polarization rotation angle $\Delta\theta$.

The solid arrows in Fig. 2 are the wave vectors while the dashed arrows denote the electric fields corresponding to the incident wave \mathbf{E}_o , the transmitted wave \mathbf{E}_T , the object-reflected wave \mathbf{E}_{R2} , and the surface-reflected wave \mathbf{E}_{R1} which is modified by a small polarization-rotated component $\delta\mathbf{E}$. The electric field can be written as,

$$\hat{\mathbf{E}}(z) = E_0 \exp(ikz) \hat{\mathbf{e}}_x + E_{R1} \exp(-ikz) \hat{\mathbf{e}}_x + \delta\mathbf{E} \exp(-ikz) \hat{\mathbf{e}}_y, \quad (z < 0) \quad (9a)$$

$$\begin{aligned} \hat{\mathbf{E}}(z) = & E_T^+ \exp(ik_+ z) \hat{\mathbf{e}}_+ + E_T^- \exp(ik_- z) \hat{\mathbf{e}}_- + \\ & E_{R2}^+ \exp(-ik_+ z) \hat{\mathbf{e}}_+ + E_{R2}^- \exp(-ik_- z) \hat{\mathbf{e}}_-, \end{aligned} \quad (0 < z < h) \quad (9b)$$

where $\hat{\mathbf{e}}_\pm = (\hat{\mathbf{e}}_x \pm i \hat{\mathbf{e}}_y) / \sqrt{2}$, $\hat{\mathbf{e}}_x$ and $\hat{\mathbf{e}}_y$ are unit vectors in the x and y direction respectively, $k = \omega/c$ is the wavenumber in air, $n_\pm = ck_\pm / \omega = \sqrt{\epsilon_o \pm \epsilon_i}$ is the complex index of refraction in magnetized water, and $\epsilon_i = (\epsilon_o - 1)\omega\Omega/D(\omega)$. Application of the electromagnetic boundary conditions yields for the configuration shown in Fig. 2 the following ratio for the polarization-rotated field,

$$\frac{\delta E}{E_0} = -i \left(\frac{n_+ \cos(k_+ h)}{n_+ \cos(k_+ h) - i \sin(k_+ h)} - \frac{n_- \cos(k_- h)}{n_- \cos(k_- h) - i \sin(k_- h)} \right). \quad (10)$$

In the limit that $h \rightarrow \infty$, the reflected Faraday rotation effect vanishes and the polarization rotation is due solely to SMOKE. In this limit Eq. (10) reduces to

$$\left| \frac{\delta E}{E_0} \right|_{h \rightarrow \infty} = \frac{n_+ - n_-}{(1+n_+)(1+n_-)} \approx \xi, \quad (11)$$

where $\xi \approx (n_0 - 1)(\omega \Omega_0 / \Omega_B^2) / (n_0^2 + n_0) \square 3 \times 10^{-12}$. The ratio of the fields given in Eq. (10) is shown in Fig. 3 as a function of the depth of the conducting plate h .

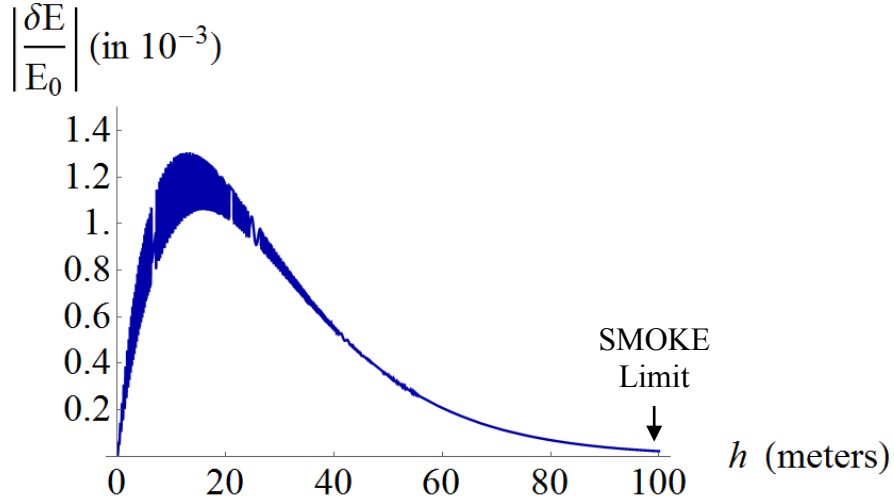


Figure 3: Ratio of the polarization-rotated reflected field to the incident field as a function of object depth h . The polarization rotation results from a combination of Faraday rotation and SMOKE; however, the contribution due to SMOKE is small.

We now consider the general SMOKE contribution to the polarization rotation by analyzing the process for arbitrary field directions. The polarization-rotated field due to SMOKE as a function of the field components of an incident plane wave, for arbitrary polarizations and angle of incidence as well as arbitrary orientation of the magnetic field, is obtained in Appendix A and found to be,

$$|\delta E| \square K(\theta) |n_B| \left(E_x^2 E_x^{*2} + 2(E_x^2 E_y^{*2} + E_x^{*2} E_y^2) \cos^2 \theta + E_y^2 E_y^{*2} \cos^4 \theta \right)^{1/4}, \quad (13)$$

where $K(\theta) \approx (\Omega_0 \omega / 10\Omega_B^2) g(\theta) = 2.5 \times 10^{-12} g(\theta) \ll 2.5 \times 10^{-12}$ and $n_B \approx (\cos \theta_B - \theta \sin^2 \theta_B \sin^2 \phi_B / 1.8) \sim 1$. In Eq. (12), θ is the angle of the incident wave vector with respect to the water's surface normal vector. The angles θ_B and ϕ_B are, respectively, the polar and azimuthal angle of Earth's magnetic field with respect to the incident wave vector, Appendix A.

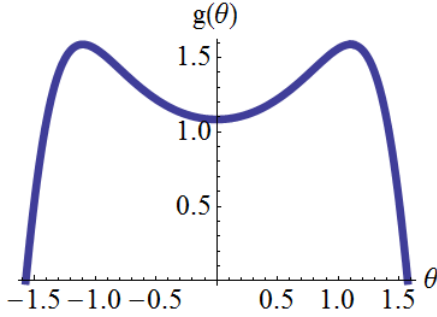


Figure 4: The function $g(\theta)$ plotted above represents the angular dependence of the polarization-rotated field on the incident wave vector's orientation for a specific geometry ($\theta_B = \phi_B = 0$, $E_y = 0$).

We find that no choice of polarization or angle of incidence will significantly increase the SMOKE contribution to the polarization rotation: see Fig. 4.

IV. Discussion

A mechanism for the remote optical detection of a shallow, i.e., $\sim 1 - 10$ m, underwater conducting object has been presented. In this mechanism, a polarized blue-green laser beam is reflected off the water's surface and the reflected, polarization-rotated electric field recorded. A variation in the measurements at two nearby locations may indicate the presence of an underwater conducting object. The polarization rotation is mainly due to the Faraday effect; SMOKE has a negligible contribution.

As an alternative to the mechanism proposed, one can detect the underwater object directly by measuring the un-rotated component of the reflected laser field. This reflected component can be significantly larger in amplitude than the polarization-rotated component. By time gating the laser pulses, the object's depth can be determined.

Acknowledgement: This work was supported by ONR, NEEC and NRL. We would like to acknowledge useful discussions with S. Potashnik.

Appendix A

A perturbative solution is described here for the polarization-rotated reflected field associated with SMOKE. The treatment allows for the incident plane wave to have arbitrary angle and polarization with respect to the water's surface and allows for arbitrary magnetic field orientation. The relevant coordinate systems are labeled in Fig. A1.

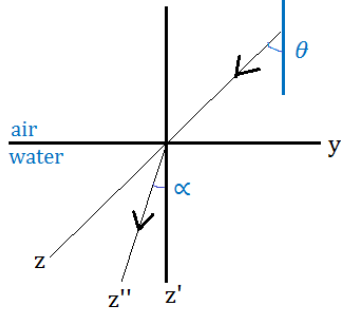


Figure A1: Coordinate systems used in the calculation of the polarization-rotated reflected field associated with SMOKE given an arbitrary geometric configuration.

The arrows correspond to the transmitted wave vector in the absence of a local magnetic field and the incident wave vector; the boundary conditions ensure that they are coplanar and that $k_0 \sin \alpha = (\omega/c) \sin \theta$, where k_0 is the magnitude of the transmitted wave vector. The coordinate systems are defined such that $x = x' = x''$ coincide.

The fields $\hat{\mathbf{E}}(\mathbf{r})$, $\hat{\mathbf{D}}(\mathbf{r})$, $\hat{\mathbf{B}}(\mathbf{r}) = -i(c/\omega)\nabla \times \hat{\mathbf{E}}(\mathbf{r})$ are expanded to first order in the small parameter $\Delta = \omega\Omega_0 / D(\omega) \ll 10^{-11}$ where, as before, $D(\omega) = \Omega_B^2 - \omega^2 - i\gamma\omega$. Since $\nabla \cdot \hat{\mathbf{D}}(\mathbf{r}) = 0$, to each order in Δ , Eq. (4) yields the wave equation $\nabla^2 \hat{\mathbf{E}}_0 + \epsilon_0(\omega^2/c^2) \hat{\mathbf{E}}_0 = 0$, where the field subscript denotes zeroth order in Δ . This wave equation is used to calculate the zeroth order field amplitudes.

For $z' > 0$, Eq. (7) implies that, for the transmitted field $\hat{\mathbf{E}}_T(\mathbf{r}) = \hat{\mathbf{E}}_{T,0}(\mathbf{r}) + \delta\hat{\mathbf{E}}_T(\mathbf{r})$,

$$(\nabla^2 + \omega^2 \epsilon_0 / c^2) \delta\hat{\mathbf{E}}_T(\mathbf{r}) = i(\epsilon_0 - 1) \omega (\mathbf{\Omega}_0 \times \bar{\nabla}) (\bar{\nabla} \times \hat{\mathbf{E}}_{T,0}(\mathbf{r})) / (\epsilon_0 D(\omega)) \quad (13)$$

The field is rewritten as $\delta\hat{\mathbf{E}}_T(\mathbf{r}) = \hat{\Gamma}(\mathbf{r}) \exp(ik_0 z'') = \Gamma(\mathbf{r}) \hat{\mathbf{e}}_\Gamma \exp(ik_0 z'')$ in order to employ the paraxial approximation $\nabla^2 \rightarrow -k_0^2 + 2ik_0 \partial / \partial z''$, which states that the field varies a negligible

amount for transverse displacements $\Delta\mathbf{r}_\perp$ on the order of a wavelength. The boundary conditions dictate that $\Gamma(\mathbf{r})$ has no x' or y' dependence at $z'=0$, i.e. $\Gamma(\mathbf{r})=\Gamma(z')$. Applying the paraxial approximation to Eq. (13) and integrating over the coordinate z' , one obtains $\Gamma(z')=a+bz'$. The constant of integration a is determined by the continuity of the magnetic field $\hat{\mathbf{B}}=-i(c/\omega)(\nabla\times\hat{\mathbf{E}})$ at the boundary. Simplification of the expression for $\sqrt{|a|^2}$ yields $|\delta\hat{\mathbf{E}}_T(z'=0)|$, i.e. $|\delta E|$ as given by Eq. (12).

References

- [1] D. Budker, W. Gawlik, D.F. Kimball, S.M. Rochwester, V.V. Yashchuk and A. Weis, Rev. Mod. Phys. **74**, 1154 (2002).
- [2] *Optical Magnetometry*, D. Budker and D.F.J. Kimball (eds.) (Cambridge University Press, Cambridge, UK, 2013).
- [3] G. Bison, R. Wynands, and A. Weis, Appl. Phys. B Lasers Opt. **76**, 325 (2003).
- [4] J.P. Davis, M.B. Rankin, L.C. Bobb, C. Giranda, M.J. Squicciarini, "REMAS Source Book," Mission and Avionics Tech. Dept., Naval Air Development Center (1989).
- [5] Luke A. Johnson, Phillip Sprangle, Bahman Hafizi, and Antonio Ting. Remote atmospheric optical magnetometry. Journal of Applied Physics, 116(6), (2014).
- [6] Z. Qiu and S. Bader, Review of Scientific Instruments **71** (3), 1243-1255 (2000).
- [7] K. Oughstun and R. Albanese, "Magnetic field contribution to the Lorentz model," J. Opt. Soc. Am. A 23, 1751-1756 (2006).
- [8] J. D. Jackson, *Classical electrodynamics*. (Wiley, New York, 1999).
- [9] Andrei, Eva. 2015. Faraday Rotation [pdf]. Retrieved from:
<http://www.physics.rutgers.edu/grad/506>

